

Nanometer Voids Prevent Crack Growth in Polymeric Materials

Cédric Dutriez,[†] Kotaro Satoh,[‡] Masami Kamigaito,[‡] and Hideaki Yokoyama^{*,†}

Nanotechnology Research Institute, National Institute of Advanced Industrial Science and Technology, Central 5, Higashi, 1-1-1, Tsukuba, Ibaraki 305-8565, Japan, and Department of Applied Chemistry, Graduate School of Engineering, Nagoya University, Furo-cho, Chikusa-ku, Nagoya 464-8603, Japan

Received June 6, 2007

Revised Manuscript Received August 29, 2007

The effect of micrometer (1–10 μm) voids in the mechanical properties of polymeric materials was studied in the 1980s and 1990s with the expectation that such small voids may initiate crazing, the toughening mechanism in polymer solids, and make the material tough similar to the function of dispersed rubber particles widely used in industry.^{1–3} However, the micrometer voids showed only limited resistance against crack growth,^{4,5} and it was concluded that much smaller voids are necessary for the drastic change in mechanical properties.⁴ We have recently succeeded in the introduction of nanometer voids into polymeric materials using the CO₂ process and block copolymer template. A block copolymer, a block of which has affinity to CO₂, was heterogeneously swollen under CO₂ pressure and then depressurized to create nanometer voids in every CO₂-philic (spherical) domain, as illustrated in Figure 1 and explained in our previous reports.^{6–9} For this study, we used poly(methyl methacrylate-*b*-perfluorooctylethyl methacrylate) (PMMA–PFMA)^{10,11} with a weight fraction of the fluorinated block of 37.1% (di40) and a molecular weight of 79 000 Da. Since the voids are introduced into the embedded spherical PFMA domains, almost no voids were observed on the films surface. We etched the thin films with reactive ions to expose the embedded voids to the surface to be visualized by scanning electron microscopy (SEM). An SEM image of such nanometer voids in the film supported on silicon wafer is shown in Figure 2. The diameter of the voids is ~ 50 nm for di40 with the optimized process condition (5 °C and 30 MPa) for the highest porosity. The successful introduction of voids is also confirmed by the increased film thickness and reduced refractive index. By assuming that the increment of the volume (thickness) is solely due to the volume of the introduced voids, porosity can be estimated as

$$p = \frac{t_f - t_i}{t_f} \quad (1)$$

where t_i and t_f are the initial and final thicknesses, respectively. Several process parameters influence the size and the number density of the voids. Among those, the pressure and temperature of CO₂ are the major factors. Similar to polystyrene-based copolymers, poly(styrene-*b*-perfluorooctylethyl methacrylate)^{6–8} and poly[styrene-*b*-4-(perfluorooctylpropyl-oxy)styrene],⁹ nanometer voids were successfully introduced into a PMMA-based block copolymer, PMMA–PFMA.

* Corresponding author. E-mail: yokoyama@ni.aist.go.jp.

[†] National Institute of Advanced Industrial Science and Technology.

[‡] Nagoya University.

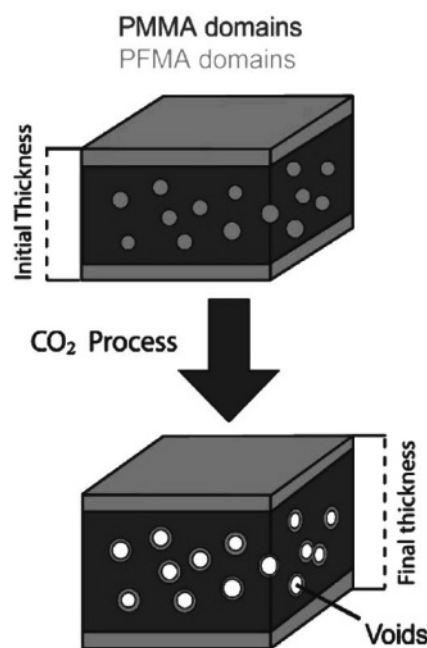


Figure 1. Schematic pictures of the CO₂ process. The CO₂-philic nanodomains in the diblock copolymer film are swollen by CO₂ and create nanometer voids after depressurization.

We analyzed the Young's modulus of the thin films using the strain-induced elastomer buckling instability mechanical measurement (SIEBIMM), developed by a group in NIST.^{12,13} The SIEBIMM consists of transferring a thin film onto a PDMS sheet under a small tensile strain (around 3%) followed by strain release. When the strain is released, the film on the PDMS sheet buckles under compressive strain. The buckling wavelength (d) is related to the modulus (E_{PDMS}) and the Poisson ratio (ν_{PDMS}) of the PDMS sheet, and to the thickness (h), the Young's modulus (E_{film}) and the Poisson ratio (ν_{film}) of the film:

$$E_{\text{film}} = E_{\text{PDMS}} \left(\frac{d}{\alpha h} \right)^3 \quad (2)$$

α is related to the Poisson ratios of PDMS and the film as

$$\alpha = 2\pi \left(\frac{(3 - \nu_{\text{PDMS}})(1 + \nu_{\text{film}})}{12} \right)^{1/3} \quad (3)$$

Equation 2 holds under the condition that thickness of the film is much smaller than that of the PDMS sheet. The Poisson ratios were assumed to be 0.33 and 0.5 for the film and the PDMS sheet, respectively. E_{PDMS} was independently estimated by dynamic viscoelastometry to a value around 2 MPa.

Figure 3 shows the evolution of the Young's modulus as a function of the porosity of the films of di40. Prior to the CO₂ process, the Young's modulus is around 1.95 GPa. As the porosity increases to 27%, the moduli of the films decrease to some value around 0.8–1.2 GPa. It should be noted that the modulus remains relatively high after the CO₂ process, which is suggestive of the film being still glassy after introduction of nanometer voids. Roberts and Garboczi¹⁴ simulated the influence of porosity on the Young's modulus of materials with several different void structures using the finite element method (FEM). Our experimental data are reasonably close to the randomly distributed spherical void model, which predicts the lowest

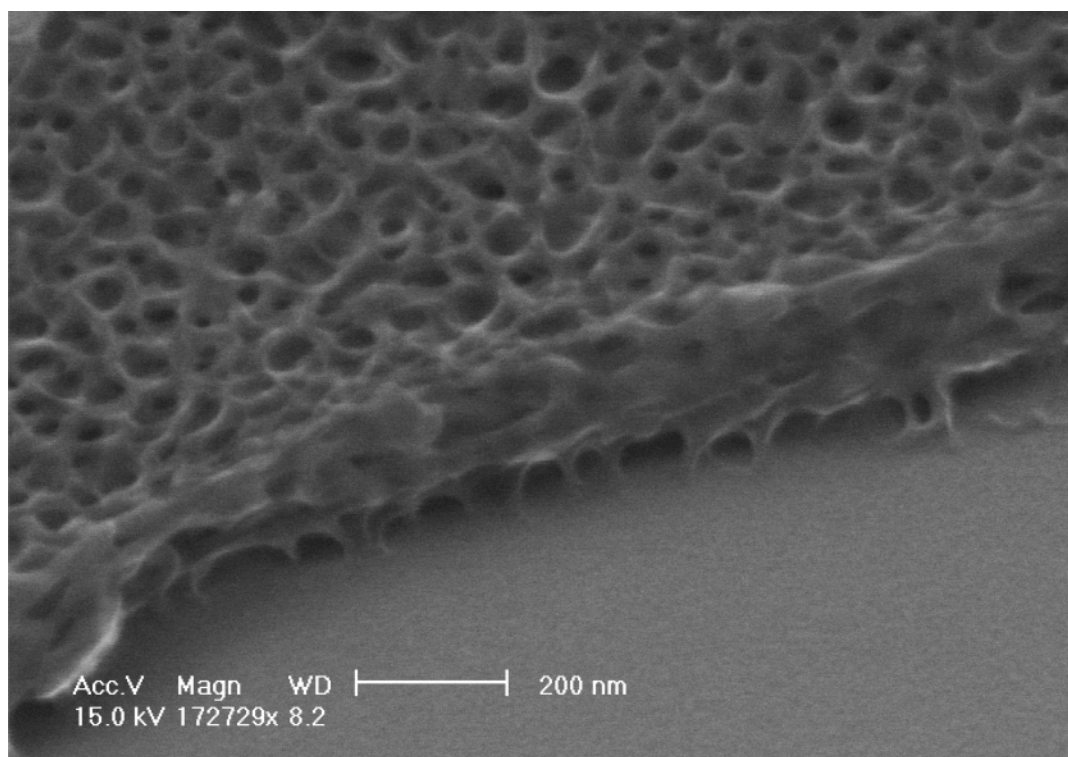


Figure 2. An SEM image of the void structure in di40 after the CO₂ process. The embedded structure was exposed to the surface by plasma etching for an SEM observation.

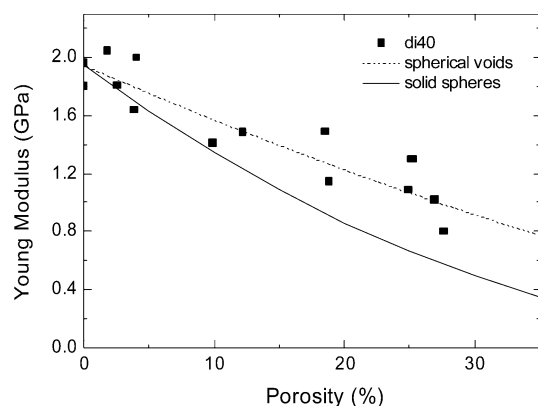


Figure 3. Effect of the porosity on the modulus of Di40 copolymer films measured by SIEBIMM. The porosity was estimated from the change of thicknesses before and after the CO₂ process. Simulation curves are extracted from the work of Roberts and Garboczi.¹⁵ Solid and dotted curves represent aggregated solid spheres and spherical voids, respectively.

impact on the Young's modulus. Since our nanometer voids are short-range ordered and have no macroscopic connectivity of voids, the impact of porosity on the Young's modulus is not catastrophic. It is important to note that the change of modulus is still reasonably predicted by the model based on continuum mechanics.

In order to estimate the elongations at break and fracture behaviors of the thin films with and without nanometer voids, we have developed a new method: imaging analysis on elastomer sheet under strain (IAES). The films under test were placed on a PDMS sheet, and the PDMS sheet was stretched. The friction between the thin film and PDMS sheet is large enough to transfer the strain from the PDMS sheet to the thin film ($\gamma_{\text{film}} = \gamma_{\text{PDMS}}$). A copper grid has often been used to support a thin film but is not used in our study since the applicable strain is not large enough to introduce macroscopic

cracks or even microscopic cracks, which will be shown later in this communication, into the films. In order to emphasize the effect of nanometer voids on the fracture, two thin films with and without nanometer voids were placed side by side on the same PDMS sheet (adhesion strengths should be the same for both films). Then strain was applied as shown in Figure 4a–c. On panels a–c, the left and right sides of the pictures are the films without (as-cast block copolymer film) and with the nanometer voids (after the process), respectively. The as-cast film (left) under strain shows the catastrophic fracture (rapid propagation of numerous cracks) in the direction perpendicular to the tensile strain even at a strain of 2.5%. Contrarily, the films with nanometer voids show no crack across the films even at 12.5% of strain. Moreover, the film with voids surprisingly did not fail even at 52.5%, a maximum strain attainable by our stretching device. We can notice that less than 100 nm thick films show no crack propagation. That may be explained by the effect of adhesion of the films to PDMS. Brown and Yang¹⁵ had shown a threshold thickness for supported polymer films on the crack elongation speed. To avoid this uncertainty, our experiments employed the films thicker than 250 nm. During the experiment, because of the Poisson ratio of the PDMS different from our films, the films buckle in the direction normal to the stretching direction. The estimated buckling wavelength of the films (measured using SIEBIMM) is from 10 to 20 μm , and the amplitude less than 2 μm . Therefore, the films is considered to be a flat film in the length scale of the 50 nm voids, and such a buckling is not likely to interfere with the crack growth mechanism. During the process to introduce nanovoids into the films, CO₂ is also absorbed into the PMMA matrix. The plasticizing effect of CO₂ is not negligible and may influence the mechanical properties. To eliminate the plasticizing effect of CO₂ on the PMMA matrix, the IAES experiment was performed at least 3 days after the CO₂ process, which is sufficient for CO₂ to evaporate completely from the films.

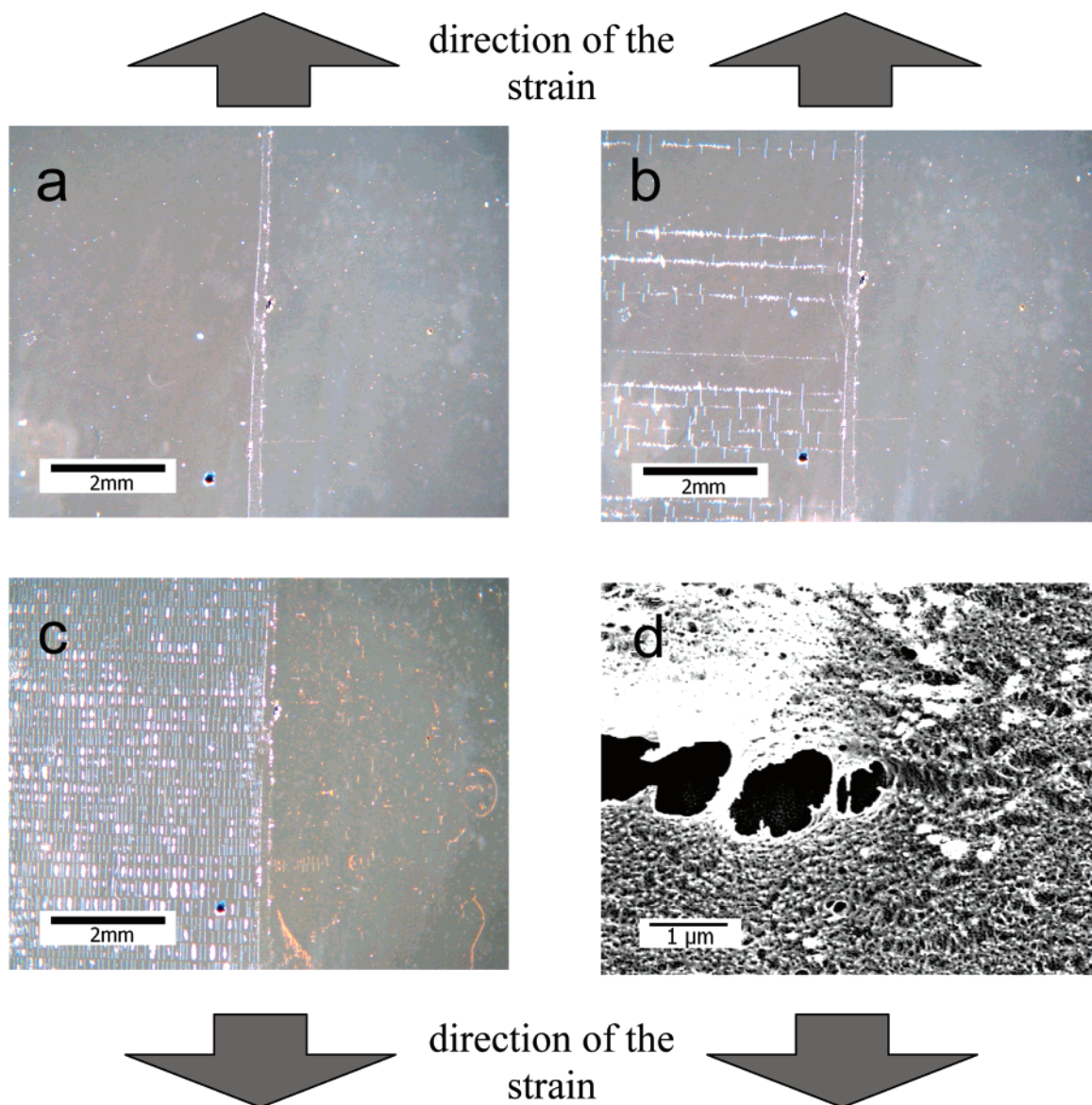


Figure 4. Observation of the 250 nm thick Di40 films unprocessed (left half of the images of a, b, and c) and with nanometer voids (right half of the images of a, b, and c) under (a) 1%, (b) 2.5%, and (c) 12.5% of strains. Horizontal cracks (perpendicular to the direction of strain) start to appear at 3% of strain for unprocessed films. No macroscopic cracks appeared up to 52.5% in the films with voids. White vertical lines in panels b and c are related to buckling and peeling of the film from the elastomer substrate initiated from the cracks due to compressive strain in the perpendicular direction. An SEM image of the tip of an isolated microscopic crack sporadically appearing in thin films with nanometer voids under 52.5% of strain is shown in panel d.

Although no failure was observed under 52.5% of strain, isolated microscopic cracks were found occasionally. Such a film on a PDMS sheet under strain was fixed onto a rigid frame and detached from the stretching device for an SEM observation. The film was etched with reactive ions to expose embedded voids and then coated with Au to prevent electronic charge-up. An example of SEM images of the microscopic crack tips is shown in Figure 4d. The structure near the crack tip shows that nanovoids in the vicinity are strongly stretched. Our block copolymer is mainly composed of PMMA, a typical brittle polymer, which catastrophically fails with rapid propagation of crack at a small strain similar to the unprocessed block copolymer films. The energy associated with the stress concentration to the crack tip is dissipated by the nanometer voids. Although no clear boundary of craze zone is found, we can notice the similarity in sizes of the nanostructure in the films and of the fibrils of crazes in the literature.¹⁶ Van Melick et al. simulated¹⁷ fracture of polystyrene with nanometer voids and

found the interparticle (intervoid) distance threshold of 15 nm for the brittle-to-ductile transition. Although our copolymer is not polystyrene-based and quantitative comparison is not appropriate, it should be noted that the voids with a diameter of ca. 50 nm and the walls thickness of 20 nm or less in our experiment are similar to the model showing ductile behavior in the simulation. The energy associated with stress concentration due to the crack tip is dissipated by stretching and breaking the walls separating the nanometer voids. We can conclude that the crack propagation in films with nanometer voids is effectively prevented although the fracture mechanism has not been revealed clearly.

The effect of nanometer voids on the mechanical properties was investigated. The SIEBIMM experiments applied on thin films with ordered nanometer voids revealed that nanometer voids have a minimum impact on the Young's modulus of the film. However, such nanometer voids change their fracture behavior. The void structure fabricated by foaming of CO₂ in

PFMA(CO₂-philic) domains of PMMA–PFMA block copolymer provides an architecture that can dissipate energy and prevent catastrophic breakdown by delaying crack propagation even in a brittle PMMA-based matrix. Voids prevent crack growth and failure when their size is reduced to nanometers.

Acknowledgment. We thank the financial support and fellowship from the Project on Nanostructured Polymeric Materials by the New Energy and Industrial Technology Development Organization.

Supporting Information Available: Description of the material and experimental methods. This material is available free of charge via the Internet at <http://pubs.acs.org>.

References and Notes

- (1) Bucknall, C. B. In *Toughened Plastics*; Applied Science Publishers: London, 1977.
- (2) Bubeck, R. A.; Buckley, D. J.; Kramer, J. E.; Brown, H. R. *J. Mater. Sci.* **1991**, *26*, 6249–6259.
- (3) Borggreve, R. J. M.; Gaymans, R. J.; Eichenwald, H. M. *Polymer* **1989**, *30*, 78–83.
- (4) Collias, D. I.; Baird, D. G. *Polym. Eng. Sci.* **1995**, *35*, 1167–1177.
- (5) Youn, R. J.; Suh, N. P. *Polym. Compos.* **1985**, *6*, 175–180.
- (6) Yokoyama, H.; Li, L.; Nemoto, T.; Sugiyama, K. *Adv. Mater.* **2004**, *16*, 1542–1546.
- (7) Li, L.; Yokoyama, H.; Nemoto, T.; Sugiyama, K. *Adv. Mater.* **2004**, *16*, 1226–1229.
- (8) Li, L.; Nemoto, T.; Sugiyama, K.; Yokoyama, H. *Macromolecules* **2006**, *39*, 4746–4755.
- (9) Yokoyama, H.; Sugiyama, K. *Macromolecules* **2005**, *38*, 10516–10522.
- (10) Hamasaki, S.; Sawauchi, C.; Kamigaito, M.; Sawamoto, M. *J. Polym. Sci., Part A: Polym. Chem.* **2002**, *40*, 617–623.
- (11) Kamigaito, M.; Ando, T.; Sawamoto, M. *Chem. Rev.* **2001**, *101*, 3689–3745.
- (12) Stafford, C. M.; Harrison, C.; Beers, K. L.; Karim, A.; Amis, E. J.; Vanlandingham, M. R.; Kim, H. C.; Volksen, W.; Miller, R. D.; Simonyi, E. E. *Nat. Mater.* **2004**, *3*, 545–550.
- (13) Stafford, C. M.; Guo, S.; Harrison, C.; Chiang, M. Y. M. *Rev. Sci. Instrum.* **2005**, *76*, 062207.
- (14) Roberts, A. P.; Garboczi, E. J. *Proc. R. Soc. London, A* **2002**, *458*, 1033–1054.
- (15) Brown, H. R.; Yang, A. C. M. *J. Mater. Sci.* **1990**, *25*, 2866–2868.
- (16) Donald, A. M.; Chan, T.; Kramer, E. J. *J. Mater. Sci.* **1981**, *16*, 669–675.
- (17) Van Melick, H. G. H.; Govaert, L. E.; Meijer, H. E. H. *Polymer* **2003**, *44*, 457.

MA071262P